

# Al<sub>0.3</sub>Ga<sub>0.7</sub>As/GaAs HEMT's Under Optical Illumination

Alvaro A. de Salles, *Member, IEEE*, and Murilo A. Romero

**Abstract**—Theoretical and experimental work for the dc and RF performance of depletion mode Al<sub>0.3</sub>Ga<sub>0.7</sub>As/GaAs HEMT's under optical illumination is presented. Photoconductive effect increasing the 2-DEG channel electron concentration and photovoltaic effect in the gate junction are considered. Optical tuning of a 2 GHz HEMT oscillator and optical control of the gain of a 2 to 6 GHz HEMT amplifier are presented and potential applications are described.

## I. INTRODUCTION

THE DIRECT optical illumination of microwave semiconductor devices has been an area of growing interest, since various RF control functions such as gain control of amplifiers, oscillator tuning, locking and frequency modulation, as well as switching, mixing, limiting and phase shifting can be achieved [1], [2]. Although some authors (e.g., [3]–[6]) have studied the optical effects in MESFET's, there is a lack of theoretical and experimental work describing the effects of illumination of HEMT's. These are very important microwave devices, since they present extremely low noise performance at frequencies up to several tens of GHz. Also, because they employ heterostructures using III–V semiconductors, they are very convenient for use in microwave monolithic integrated circuits (MMIC's) or optoelectronic integrated circuits (OEIC's).

A detailed analysis considering all the effects resulting from optical illumination of HEMT's is a very complex task. However, by making some assumptions, a simplified analysis considering the relevant photoeffects can be made [7]. In this paper, a simplified analysis to account for the photoconductive and the photovoltaic effects is described and from this the change in the dc and RF performance with illumination are estimated. Also, experiments showing optical tuning of a 2 GHz HEMT oscillator and

Manuscript received April 10, 1991; revised July 29, 1991. This work was supported in part by TELEBRAS under contract PUC-TELEBRAS No. 293-88 and by CNPq-Brazilian Research Council/RHAE Program.

The authors were with the Center for Studies in Telecommunications, Catholic University of Rio de Janeiro, Rua Marquês de São Vicente 225, Gávea, 22453, Rio de Janeiro, RJ, Brazil. A. A. de Salles is presently with the Federal University of Rio Grande do Sul, Electrical Engineering Department, Rua Sarmento Leite esq., Av. Osvaldo Aranha, CEP 90210, Porto Alegre, RS, Brazil. M. A. Romero is presently with Drexel University, Philadelphia, PA 19104.

IEEE Log Number 9103990.

optical control of gain of a 2 to 6 GHz HEMT amplifier are presented. The FHR01FH AlGaAs/GaAs HEMT's from Fujitsu ( $L = 0.5 \mu\text{m}$ ) without the cover cap were used. The circuits were developed on Rogers 6010 substrates ( $H = 0.635 \text{ mm}$ ;  $\epsilon_r = 10.6$ ) including a high gate bias resistance ( $R_g = 1.2 \text{ M}\Omega$ ). Illumination was provided from a model 155 HeNe laser ( $\lambda = 632.8 \text{ nm}$ ) from Spectra Physics, focused with a X25/0.50 microscope objective.

## II. RELEVANT PHOTOEFFECTS

Fig. 1 shows the band diagram of a typical depletion mode Al<sub>0.3</sub>Ga<sub>0.7</sub>As/GaAs HEMT under illumination with photon energy  $E_{ph} = h\nu = hc/\lambda$  from the top. The following assumptions will be made:

- 1) pumping of electrons from gate metal into AlGaAs layer is negligible;
- 2) pumping of electrons from the 2 DEG channel into the AlGaAs layer is negligible;
- 3) trapping center densities in the semiconductor surface and in the AlGaAs and GaAs layers are very close to the conduction band edge and therefore present negligible effects at room temperature.

Then, the major photoeffects arising in the illumination of AlGaAs/GaAs HEMT's are band-to-band photon absorption in the GaAs and in the AlGaAs layer, generating hole-electron pairs in these regions (Fig. 1).

When photons are absorbed only in the GaAs layer, an increase in the electron concentration of the 2-DEG channel occurs (photoconductive effect). When photons are also absorbed in the AlGaAs layer and a high-gate bias resistance is present, the photovoltaic effect is dominant. The relevant dimensions and material properties of the HEMT considered are presented in Table I. The Au-Al<sub>0.3</sub>Ga<sub>0.7</sub>As/GaAs Schottky barrier height is of the order of 1.11 V [8].

## III. PHOTOCODUCTIVE EFFECT

The photoconductive effect is dominant when the incident photon energy  $E_{ph} = h\nu$  is equal to or greater than the GaAs bandgap but smaller than the AlGaAs bandgap ( $E_{g1} \leq E_{ph} < E_{g2}$ ). Then the AlGaAs layer is transparent

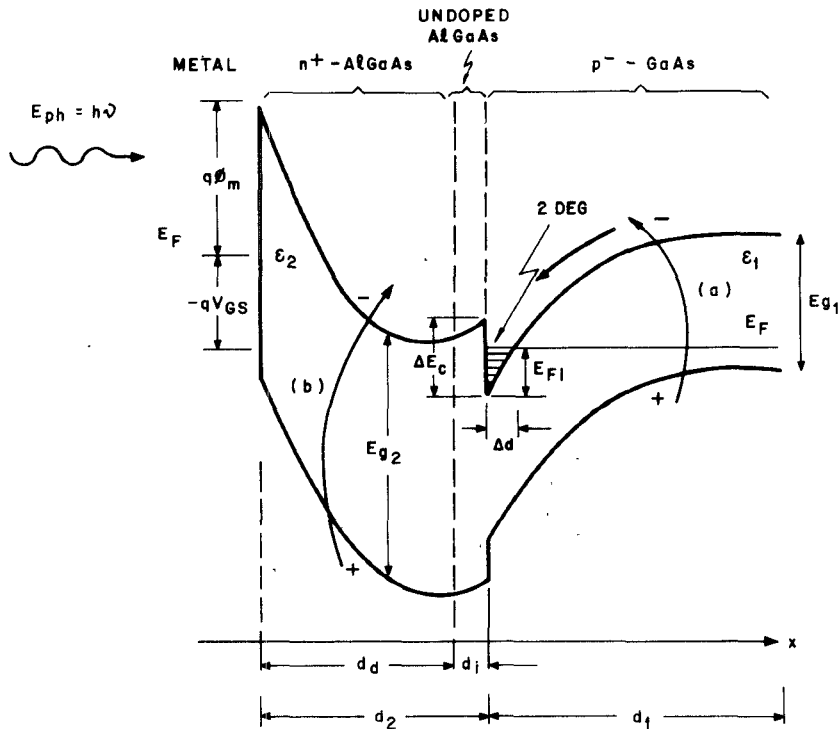


Fig. 1. Hole-electron pairs photoexcited in the AlGaAs and GaAs layers.

TABLE I  
RELEVANT DIMENSIONS AND MATERIAL PROPERTIES OF THE HEMT CONSIDERED IN THIS ANALYSIS

Material	Doping Density ( $\text{cm}^{-3}$ )	Thickness $d$	Optical Absorption Coefficient $\alpha$ ( $\text{cm}^{-1}$ )	Bandgap (eV) ( $T = 300 \text{ K}$ )	Intrinsic Carrier Concentration $n_i$ ( $\text{cm}^{-3}$ )	Minority Carrier Lifetime $\tau$ (s)	Relative Permittivity $\epsilon$
1) aAs	$1 \times 10^{14}$	$0.2 \mu\text{m}$	$1 \times 10^4$	1.424	$1.79 \times 10^6$	$10^{-8}$	13.1
2) $\text{Al}_{0.3}\text{Ga}_{0.7}\text{As}$	$1 \times 10^{18}$	$525 \text{ \AA}$	$1.25 \times 10^4$	1.8	$2.5 \times 10^3$	$10^{-9}$	12.1

$Z = 200 \mu\text{m}$ ;  $L = 0.5 \mu\text{m}$ ;  $\Delta d = 80 \text{ \AA}$ ;  $\Delta E_c = 0.32 \text{ eV}$ ;  $\mu = 6800 \text{ cm}^2/\text{V.s}$ ;  $v_s = 2 \times 10^7 \text{ cm/s}$ ;  $d_i = 20 \text{ \AA}$ .

to the illumination and the dominant photoeffect is the generation of hole-electron pairs in the GaAs layer, if it is thick enough. Because the GaAs layer has a low doping level, the heterojunction depletion region extends deeply into this layer; therefore most of the optical absorption occurs in a nonzero field region. This improves quantum efficiency and eliminates the slow diffusion process. Photoelectrons generated in this layer will experience a vertical field associated with the band bending of the heterojunction, as shown in Fig. 1 and a horizontal field associated with the applied drain-to-source voltage. Since the electrons travelling in the vertical direction will be collected by the 2-DEG layer, all the photoelectrons, generated in the GaAs layer will contribute to increase the HEMT output conductance and source-to-drain current. The photogenerated holes drifting towards the semi-insulating substrate will be capacitively coupled into the grounded source, if it is an ac signal. These holes, as well as those drifting towards the source due to the positive drain bias will induce electrons which are supplied by the source, completing therefore the current path.

An estimation of the increase in the electron concentration  $n_{sph}$  in the 2-DEG channel due to illumination can be made as follows. The photoelectron density generated in the GaAs layer when  $\alpha_1 d_1 \ll 1$  and assuming that the quantum efficiency is unity is expressed as [9], [10]

$$\Delta n = \frac{\tau_n}{d_1} \cdot \frac{S_{\text{opt}} \cdot \lambda}{hc} \cdot (1 - e^{-\alpha_1 d_1}), \quad (1)$$

where  $h$  is Planck's constant,  $S_{\text{opt}}$  is the incident optical power density,  $\lambda$  is the incident optical wavelength,  $\alpha_1$  the GaAs optical absorption coefficient,  $d_1$  is the thickness of the GaAs layer,  $\tau_n$  is the electron lifetime and  $c$  is the speed of light in vacuum. Then, the electron concentration  $n_{sph}$  in the 2-DEG channel due to illumination can be estimated from (1) as

$$n_{sph} = \Delta n \cdot d_1 = \tau_n \cdot \frac{S_{\text{opt}} \cdot \lambda}{hc} \cdot (1 - e^{-\alpha_1 d_1}). \quad (2)$$

Expression (2) assumes that the variation of the photoelectron concentration  $n_{sph}$  with the small signal change of the gate bias voltage  $V_{GS}$  is negligible. Now, assuming

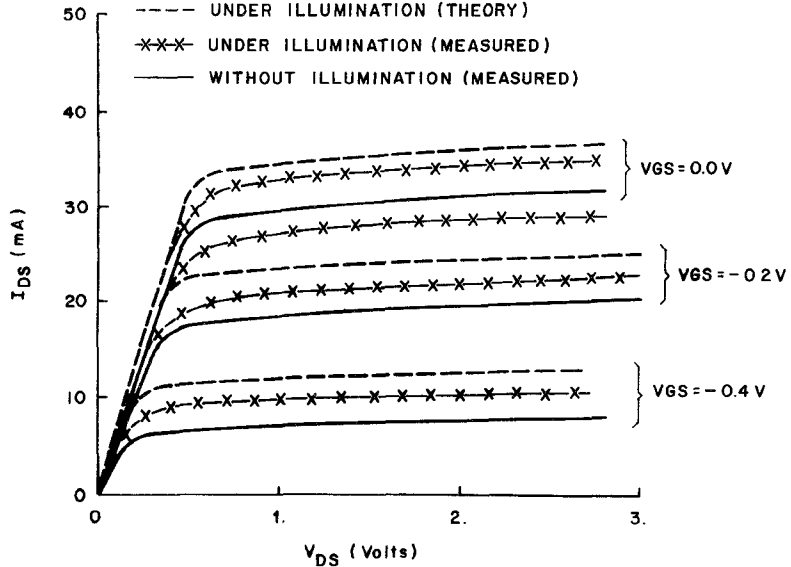


Fig. 2. Estimated and measured I-V characteristics due to photoexcitation of carriers in the GaAs layer (photoconductive effect).

that the photoelectrons drift at the saturated velocity  $v_s$  in the 2-DEG channel, the drain-to-source photocurrent  $I_{DS_{ph}}$  can be estimated from

$$I_{DS_{ph}} = Z \cdot q \cdot n_{sph} \cdot v_s, \quad (3)$$

and the overall drain-to-source current under illumination is

$$I_{DSi} = I_{DS} + I_{DS_{ph}} = Z \cdot q \cdot v_s \cdot (n_s + n_{ph}) = Z \cdot q \cdot v_s \cdot n_{si}, \quad (4)$$

where  $I_{DS}$  and  $n_s$  are the drain-to-source current and the 2-DEG channel electron density without illumination respectively and  $n_{si}$  is the 2-DEG channel electron density under illumination. Fig. 2 shows a comparison between the estimated and measured photocurrent due to the photoconductive effect in the GaAs layer. The HEMT parameters are given in Table I and an incident optical power ( $E_{ph} = 1.43$  eV) of 0.2 mW focused to a 50  $\mu\text{m}$  diameter spot gives an optical power density  $S_{opt}$  at the heterojunction of the order of  $S_{opt} = 10 \text{ W/cm}^2$ .

Hence (2) gives  $n_{sph} = 0.8 \times 10^{11} \text{ electrons/cm}^2$  and (3) gives  $I_{DS_{ph}} = 5 \text{ mA}$ , which is in very close agreement with the experiments (Fig. 2).

#### IV. PHOTOVOLTAIC EFFECT

If the incident photon energy  $E_{ph}$  is equal to or greater than the AlGaAs bandgap ( $E_{ph} \geq E_{g2}$ ), then optical absorption and generation of hole-electron pairs may occur in both AlGaAs and GaAs layers. The relative importance of the absorption in these layers will be a function mainly of their thicknesses and of the correspondent optical absorption coefficients. When the optical power density incident in the GaAs layer is known, the increase in the 2-DEG sheet concentration and the photocurrent due to the absorption in this layer are estimated using (2)

and (3), respectively. The optical energy absorption in the AlGaAs Schottky gate depletion region produces a photovoltaic effect similar to that experienced in the Schottky gate depletion region of the MESFET's. The effects of this photovoltage in the dc and RF characteristics of the HEMT's, as it occurred in the case of the MESFET's [3], will be, among others, a close function of the gate-bias voltage and of the gate-bias resistance. When a high gate-bias resistance is present, then a significant photovoltage will be superimposed to the gate-bias voltage applied without illumination. The maximum value of the photovoltage developed is a function of the gate-bias voltage  $V_{GS}$ , of the junction built-in voltage  $V_{bi}$ , of the gate bias resistance  $R_g$  and of the absorbed optical power density  $S_{opt}$ . As forward bias reduces the thickness of the depletion region and therefore the optical absorbed power, a saturation effect will also limit the maximum photovoltage developed [3]. Because the polarity of the photovoltage is the same as forward biasing the gate junction, the drain-to-source current and the gate-to-source capacitance will increase with the increase of the photovoltage developed.

The transconductance increases up to a certain value with the increase of the photovoltage, and it decreases after that point, as it occurs in HEMT's without illumination. When  $\alpha_2 d_2 \ll 1$ , an estimation of the photogenerated hole concentration  $\Delta p$  can be made using the expression [4], [9]–[10],

$$\Delta p = \frac{\tau_p}{d_2} \cdot \left[ \frac{S_{opt} \cdot \lambda}{hc} \right] \cdot (1 - e^{-\alpha_2 d_2}), \quad (5)$$

where  $\tau_p$  is the minority carrier lifetime,  $\alpha_2$  and  $d_2$  are the absorption coefficient and the thickness of the AlGaAs layer, respectively. Then an estimation of the photovoltage  $V_{ph}$  generated in the gate depletion region can be

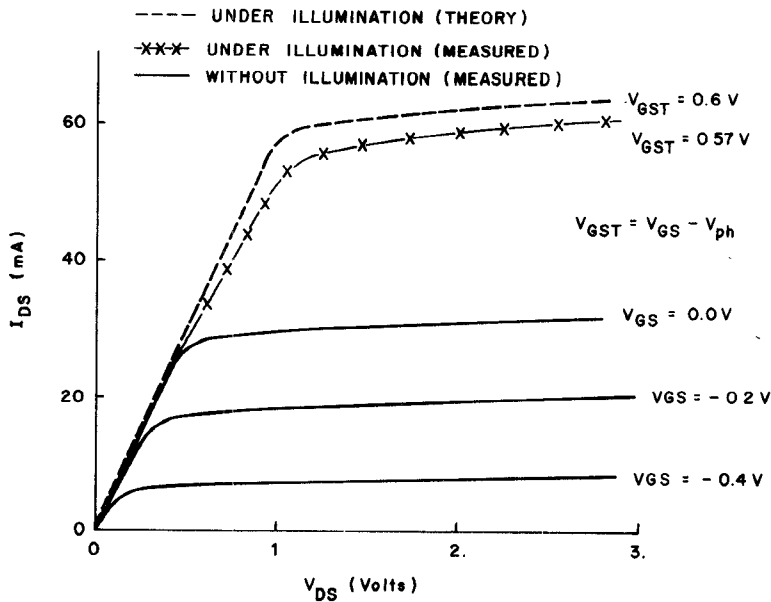


Fig. 3. Estimated and measured I-V characteristics due to photovoltaic effect in the gate junction.

made using the expression [4], [9]–[10]

$$V_{ph} = \frac{k \cdot T}{q} \cdot \ln \left( \frac{p + \Delta p}{p} \right), \quad (6)$$

where  $k$  is the Boltzmann's constant,  $p = n_i^2/n$  is the equilibrium hole concentration,  $n_i$  is the intrinsic carrier concentration and  $n$  is the carrier concentration, which is approximately equal to the donor impurity density  $N_D$  of the AlGaAs layer. For the typical parameters shown in Table I, assuming that the hole lifetime  $\tau_p$  is of the order of  $10^{-9}$  s, we obtain  $p = n_i^2/n = 6.25 \times 10^{-12} \text{ cm}^{-3}$ . When the device is illuminated with an optical power density  $S_{\text{opt}} = 10 \text{ W/cm}^2$  at  $E_{ph} = 1.8 \text{ eV}$ , (5) gives  $\Delta p = 4.2 \times 10^{14} \text{ cm}^{-9}$  when  $d_2 = 525 \text{ \AA}$ , and (6) gives  $V_{ph} = 1.55 \text{ V}$ . Since the gate junction built-in voltage is  $V_{bi} = 1.1 \text{ V}$ , at zero gate-bias voltage ( $V_{GS} = 0 \text{ V}$ ) the photovoltaic  $V_{ph}$  is limited to  $V_{ph}$  (1.1 V). However, in the experiments the photovoltaic developed was limited to typical values around 0.5–0.7 V, when  $V_{GS} \neq 0 \text{ V}$ . This is mainly due to the saturation mechanism already mentioned, since forward biasing the depletion region reduces its thickness and therefore the optical absorbed power. Then, assuming that a high resistance is connected to the gate-bias circuit, the photovoltaic effect in the HEMT gate junction is considered in the expressions for the HEMT performance without illumination; in a similar manner as for the MESFET's [3] the net voltage  $V_{GST}$  at the gate under illumination is a superposition of the gate-bias  $V_{GS}$  and the photovoltaic  $V_{ph}$  given by

$$V_{GST} = V_{GS} - V_{ph}, \quad (7)$$

since the photovoltaic  $V_{ph}$  is equivalent to forward biasing the gate junction. Fig. 3 shows a comparison between the estimated and the measured photocurrent due to the photovoltaic effect in the gate junction, when the incident optical power density  $S_{\text{opt}} = 10 \text{ W/cm}^2$  at  $E_{ph} \geq E_{g2}$  and

the gate-bias resistance is  $R_g = 1.2 \text{ M}\Omega$ . Table II shows a comparison between the applied gate-to-source voltage  $V_{GS}$ , the photovoltaic  $V_{ph}$  and the drain-to-source current  $I_{DS}$  when the gate resistance  $R_g$  has values of  $1.2 \text{ M}\Omega$ ,  $100 \text{ K}\Omega$ , and  $0 \Omega$ .

It can be seen from Table II that a photovoltaic  $V_{ph} = 0.56 \text{ V}$  is measured when  $V_{GS} = 0 \text{ V}$  and  $R_g = 1.2 \text{ M}\Omega$ . Also, as it occurred in the case of the MESFET's [3], the maximum advantage of the photovoltaic effect is obtained when the HEMT is biased close to its pinch-off condition.

## V. RF PERFORMANCE UNDER ILLUMINATION

A simplified small signal RF equivalent circuit model for the HEMT is shown in Fig. 4. According to the previous discussion, the change in some HEMT equivalent circuit elements is significantly influenced depending on the region in which the photons are absorbed and of the gate bias resistance value. When the photoconductive and the photovoltaic effects are considered to predict the change in the equivalent circuit parameters of the HEMT, then the new  $Y$  and  $S$  parameters of the intrinsic device under illumination are calculated from usual relationships.

### A. Absorption in the GaAs Layer ( $E_{g1} \leq E_{ph} < E_{g2}$ )

Expressions (2) and (3) were derived assuming that in the small signal regime the change in the 2-DEG channel photoelectron concentration  $n_{Sp}$  and therefore the change in the HEMT photocurrent  $I_{DSph}$  due to the photoconductive effect in the GaAs layer were negligible for small variations of the RF voltage applied to the gate. Therefore, as a first approximation, a negligible change in some relevant HEMT parameters are expected due to illumination. For example, the transconductance  $g_{mi}$  un-

TABLE II  
MEASURED PHOTOVOLTAGE  $V_{ph}$  AND DRAIN-TO-SOURCE CURRENT  $I_{dsi}$  FOR DIFFERENT GATE BIAS RESISTANCE  $R_g$

Under Illumination ( $R_g = 1.2 \text{ M}\Omega$ )			
$V_{gs}$ (V)	$V_{gs_t}$ (V)	$V_{ph}$ (V)	$I_{ds_t}$ (mA)
0.017	0.579	0.562	60.0
-0.200	0.561	0.761	59.5
-0.400	0.546	0.946	59.5
-0.600	0.525	1.125	59.0
-0.800	0.477	1.277	58.0
-1.000	0.400	1.400	56.0
-1.200	0.275	1.475	54.0
-1.400	0.138	1.538	51.0
Under Illumination ( $R_g = 100 \text{ K}\Omega$ )			
$V_{gs}$ (V)	$V_{gs_t}$ (V)	$V_{ph}$ (V)	$I_{ds_t}$ (mA)
0.017	0.139	0.122	51.0
-0.200	-0.069	0.131	45.0
-0.400	-0.247	0.153	37.0
-0.600	-0.420	0.180	29.0
-0.800	-0.575	0.225	20.5
-1.000	-0.715	0.285	14.5
-1.200	-0.826	0.374	9.5
-1.400	-0.917	0.483	7.0
Under Illumination ( $R_g = 0 \text{ }\Omega$ )			Dark ( $R_g = 0 \text{ }\Omega$ )
$V_{gs}$ (V)	$V_{gs_t}$ (V)	$I_{ds_t}$ (mA)	$I_{ds}$ (mA)
0.017	0.017	47.5	46.5
-0.200	-0.198	39.5	38.0
-0.400	-0.395	29.5	28.5
-0.600	-0.598	19.0	18.0
-0.800	-0.792	10.5	8.5
-1.000	-0.992	4.5	3.0
-1.200	-1.119	1.0	0.0
-1.400	-1.390	0.0	0.0

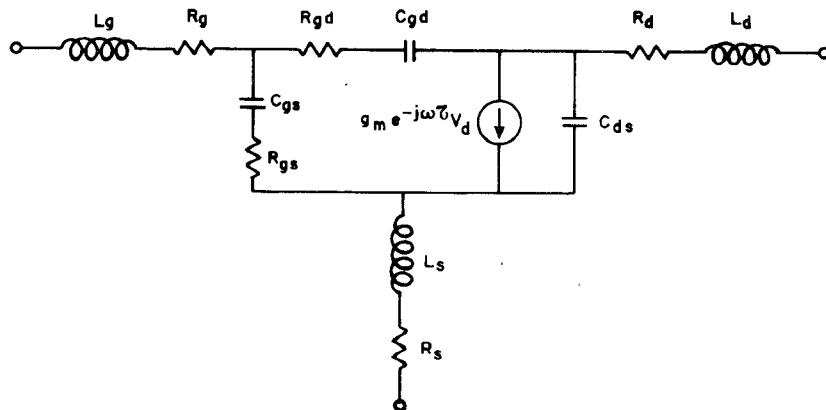


Fig. 4. Simplified small-signal RF equivalent circuit for the intrinsic HEMT.

der illumination is

$$g_{mi} = \frac{\partial I_{DSi}}{\partial V_{GS}} = \frac{\partial (I_{DS} + I_{DSph})}{\partial V_{GS}} \approx \frac{\partial I_{DS}}{\partial V_{GS}}, \quad (8)$$

which is the same as the transconductance without illumination. Also, the gate-to-source capacitance  $C_{GSi}$  under illumination is

$$C_{GSi} = q \cdot \frac{\partial (n_s + n_{sph})}{\partial V_{GS}} \cdot L \cdot Z = \frac{\partial n_s}{\partial V_{GS}} \cdot q \cdot Z \cdot L, \quad (9)$$

which also is the same as the gate-to-source capacitance  $C_{GS}$  without illumination. However, as the density of carriers in the 2-DEG channel increases with illumination

(2), the HEMT drain input impedance is expected to change since the drain-to-source resistance  $R_{DS}$  is reduced. Therefore, a negligible change in the  $S_{11}$ ,  $S_{12}$ , and  $S_{21}$  parameters and a reasonable variation in the  $S_{22}$  parameters with illumination are expected when the optical absorption is mainly in the GaAs layer. From this simplified analysis, it can be predicted that optical absorption in the GaAs layer is not convenient 1) for optical control of the gain of HEMT amplifiers, since the variation of the transconductance with illumination is not significant (8), nor 2) for optical tuning or optical injection locking of HEMT oscillators in which the gate-to-source capacitance is the frequency determining element,

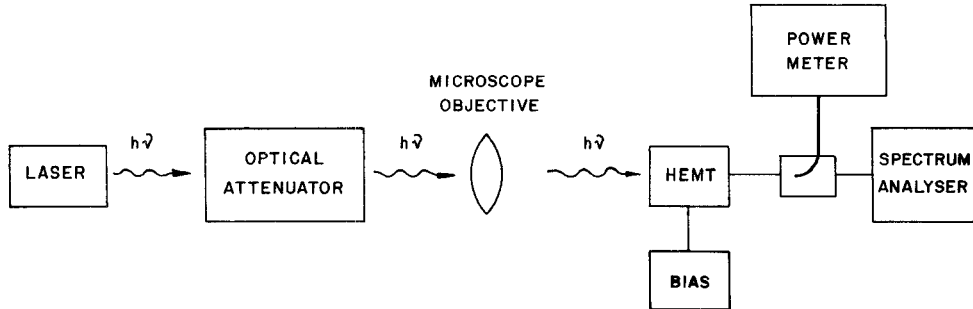


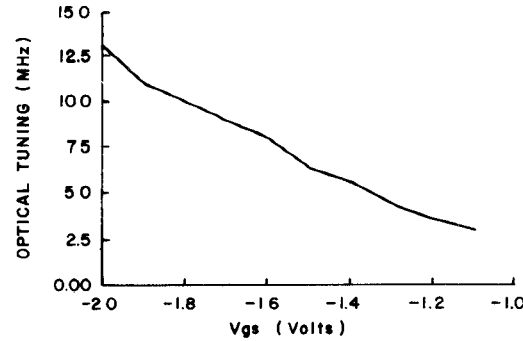
Fig. 5. Schematic diagram for the measurements.

since the variation of the gate-to-source capacitance with illumination is also negligible (9). However, the optical absorption in the GaAs layer can be of great interest for applications 1) in optical tuning or optical injection locking of HEMT oscillators in which the drain input impedance ( $S_{22}$  parameter) has a dominant effect in the frequency of oscillation and 2) in HEMT photoconductive detectors, in which the amplitude of the drain current is varied by the intensity of the optical power absorbed in the GaAs layer [11]–[14]. In this case, very wide bandwidths can be achieved (hundreds of GHz) due to the very short transit time (in the order of picoseconds) of the photocarriers. However, it should be mentioned that the predicted RF performance under illumination can be significantly degraded when slow reacting deep levels are involved in the process.

#### B. Absorption in the AlGaAs Layer ( $E_{ph} \geq E_{g2}$ )

The photovoltaic effect arising from the absorption of photons in the AlGaAs layer when a high gate-bias resistance is present is very similar to the photovoltaic effect developed in the MESFET gate junction. Thus, a variation of the HEMT RF circuit elements with illumination analogous to that experienced by the MESFET RF circuit elements under illumination [3] is expected. Because the photovoltage  $V_{ph}$  developed is equivalent to forward biasing the gate junction and since the net voltage  $V_{GST}$  at the gate under illumination is a superposition of the gate-bias voltage  $V_{GS}$  and the photovoltage  $V_{ph}$ , (7) can be used to calculate a shift in the gate bias point due to illumination. Therefore the RF circuit elements can be estimated from the expressions for the HEMT's without illumination, in which  $V_{GS}$  is replaced by  $V_{GST}$ . In this case, as a first approximation, the photoconductive effect will be assumed negligible. Hence the variation of the net gate voltage  $V_{GST}$  will produce essentially a change in the 2-DEG channel current. Then, the HEMT transconductance  $g_{mi}$  under illumination in the saturation region is a function of the net gate voltage  $V_{GST}$  and can be estimated from

$$g_{mi} = q \cdot Z \cdot v_s \cdot \frac{\partial n_{si}}{\partial V_{GST}} = \frac{q \cdot Z \cdot v_s \cdot (1 - \alpha) \cdot n_{so}}{V_1 \cdot \cosh^2 \left( \frac{V_{GST} - V_{gm}}{V_1} \right)}, \quad (10)$$

Fig. 6. Measured HEMT oscillator optical tuning range versus gate-to-source voltage  $V_{GS}$ .

in which the density of electrons  $n_{si}$  in the 2-DEG channel in function of the net gate voltage  $V_{GST}$  is given by the empirical expression [15]

$$n_{si} = n_{so} \left[ \alpha + (1 - \alpha) \tanh \left( \frac{V_{GST} - V_{gm}}{V_1} \right) \right], \quad (11)$$

where  $n_{so}$  is the maximum density of electrons in the 2-DEG channel and  $\alpha$ ,  $V_{gm}$  and  $V_1$  are parameters for curve fitting.

Also, since the gate-to-source capacitance increases with the decrease of the reverse gate-bias voltage, an increase in the gate-to-source capacitance is expected with illumination. This effect can be of great interest for optical control of HEMT oscillators in which the input capacitance is the frequency determining element. In these oscillators, illumination with photon energy equal to or greater than the AlGaAs bandgap is expected to have a significant effect in the optical tuning or in the optical injection locking of the oscillators. The gate-to-source capacitance  $C_{GSi}$  due to the photovoltaic effect in the gate junction can be estimated from

$$C_{GSi} = q \cdot \frac{\partial n_{si}}{\partial V_{GST}} \cdot L \cdot Z = \frac{g_{mi} \cdot L}{v_s}. \quad (12)$$

Once the shift in the gate-bias point  $V_{GST}$  due to photovoltaic effect is calculated, (10) and (12) can be used to estimate the transconductance and the gate-to-source capacitance under illumination, respectively. This is now used to predict the optical control performance of HEMT amplifiers and oscillators.

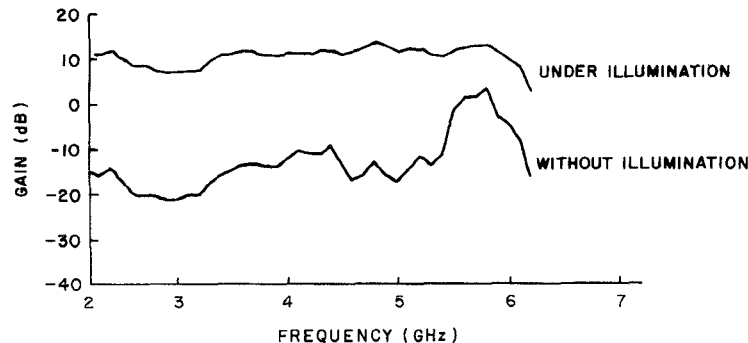


Fig. 7. Measured optical gain control of HEMT amplifier.

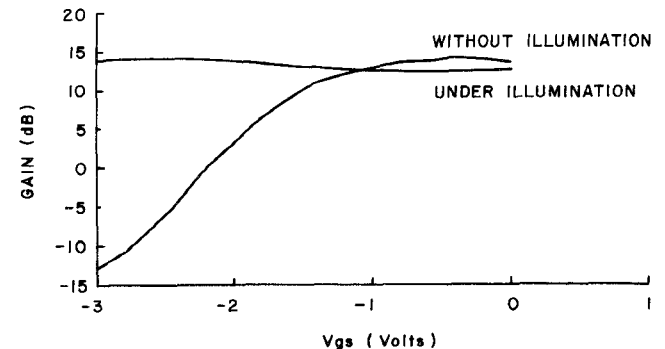
Another application, an HEMT photodetector using the photovoltaic detection mechanism may attract great interest due to its large sensitivity and moderate band width. Its major frequency limitation would be the input circuit  $RC$  time constant.

## VI. OPTICAL TUNING OF AN HEMT OSCILLATOR

A source series feedback HEMT oscillator in which the input gate circuit is the frequency determining element was developed using type FHRO1FH HEMT from Fujitsu to operate around 2 GHz. A gate bias resistance  $R_g = 1.2 \text{ M}\Omega$  was included and the incident optical power ( $E_{ph} = 1.8 \text{ eV}$ ) was varied from 0 to 0.5 mW. The schematic diagram for the measurements is shown in Fig. 5. Fig. 6 shows the optical tuning range measured at different gate-to-source bias voltage  $V_{GS}$ . The output power was around +13 dBm without illumination when the center frequency was  $F_0 = 1982 \text{ MHz}$  ( $V_{DS} = 2 \text{ V}$  and  $I_{DS} = 10 \text{ mA}$ ). The maximum variation of the output power within the measured optical tuning range was around 0.5 dB. From Fig. 6 it can be seen that around 12 MHz optical tuning range of the HEMT oscillator has been measured. This can be useful in many practical applications. Since the HEMT used was a commercially available device and therefore not optimized for efficient optical absorption in the gate depletion region, this is expected to limit the optical tuning range. The rate at which the frequency can be changed will be mainly limited by the input circuit  $RC$  time constant.

## VII. OPTICAL GAIN CONTROL OF AN HEMT AMPLIFIER

A 2–6 GHz common source HEMT amplifier including a gate-bias resistance  $R_g = 1.2 \text{ M}\Omega$  was developed to investigate the optical gain control performance ( $E_{ph} = 1.8 \text{ eV}$ ). Fig. 7 illustrates the gain without ( $P_{opt} = 0 \text{ mW}$ ) and under illumination ( $P_{opt} = 0.5 \text{ mW}$ ) when the HEMT was biased at  $V_{GS} = -3 \text{ V}$  and  $V_{DS} = 3 \text{ V}$ . It can be seen from this graph that around 31 dB of gain variation was measured at 4.7 GHz, since an attenuation of around 18 dB without illumination is varied to a gain of around 13 dB under illumination. Fig. 8 shows the variation of the HEMT amplifier gain for different values of the gate-to-source voltage  $V_{GS}$  at a frequency of 4.6 GHz, when the

Fig. 8. Measured optical gain variation of HEMT amplifier versus gate-to-source voltage  $V_{GS}$ .

drain-to-source voltage  $V_{DS} = 3 \text{ V}$ . Since the transconductance does not show a linear performance with respect to  $V_{GS}$ , the gain without illumination can be higher than the gain measured under illumination. This can be due to the parasitic MESFET operation in the AlGaAs layer of the HEMT or to surface state occupation which was not considered in this analysis.

## VIII. CONCLUSION

Photovoltaic and photoconductive effects in the AlGaAs and GaAs layers of the device were considered and the change in the dc and RF characteristics of the HEMT under illumination were predicted. The photoconductive effect was found to increase the drain-to-source current by a factor around 10 percent (at  $V_{GS} = 0 \text{ V}$ ) for the levels of illumination used. However, dramatic changes on the net gate voltage are found when the gate bias resistance is high and when the incident photon energy is equal to or larger than the AlGaAs bandgap. Under these conditions significant changes in the device transconductance and in the gate-to-source capacitance are obtained. The variation of these parameters are used to estimate the variation of the small signal  $S$  parameters of the device, and from these the performance of HEMT amplifiers and oscillators under illumination can be predicted. Experimental work using the photovoltaic effect was shown in which large control of gain (many decibels) of a 2–6 GHz HEMT amplifier and moderate tuning range (around 12 MHz) of a 2 GHz HEMT oscillator were obtained. It is

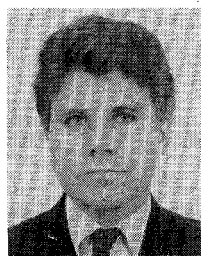
believed that those results can be improved by designing a HEMT structure for optimal optical absorption. The optical injection locking performance of HEMT oscillators need to be accessed and this may attract also great interest. The optical control techniques of HEMT's can find important applications in many modern communication systems, phased-array radars and specially in microwave monolithic integrated circuits (MMIC's) and in optoelectronic Integrated circuits (OEIC's).

#### ACKNOWLEDGMENT

The authors are grateful to some colleagues from CETUC (Center for Studies in Telecommunications from Catholic University of Rio de Janeiro), particularly to Prof. M. M. Mosso for his assistance during the experiments and A. L. Almeida Cunha. Also, the first author would like to acknowledge the hospitality of the Federal University of Rio Grande do Sul, where much of this paper was written.

#### REFERENCES

- [1] A. J. Seeds and A. A. de Salles, "Optical control of microwave semiconductor devices," *IEEE Trans. Microwave Theory Tech.*, vol. 38, no. 5, pp. 577-585, May 1990.
- [2] R. G. Hunsperger, "Optical control of microwave devices," in *Integrated Optical Circuit Engineering II*, SPIE, vol. 578, S. Sriram, Ed. Bellingham: SPIE, 1985, pp. 40-45.
- [3] A. A. de Salles, "Optical control of GaAs MESFETs," *IEEE Trans. Microwave Theory Tech.*, vol. MTT-31, no. 10, pp. 812-820, Oct. 1983.
- [4] J. Graffeuil, P. Rossel, and H. Martinot, "Light-induced effects in GaAs FETs," *Electronics Letters*, vol. 15, pp. 439-441, 1979.
- [5] R. N. Simons and K. B. Bhasin, "Analysis of optically controlled microwave/millimeter wave device structures," *IEEE Trans. Microwave Theory Tech.*, vol. MTT-34, no. 12, pp. 1346-1355, Dec. 1986.
- [6] R. N. Simons, "Microwave performance of an optically controlled  $\text{AlGaAs}/\text{GaAs}$  high electron mobility transistor and GaAs MESFET," *IEEE Trans. Microwave Theory Tech.*, vol. MTT-35, no. 12, pp. 1444-1455, Dec. 1987.
- [7] A. A. de Salles, "Optical effects in HEMTs," *Microwave and Optical Technology Letters*, vol. 3, no. 10, pp. 350-354, Oct. 1990.
- [8] J. S. Best, "The Schottky-barrier height of Au on n- $\text{Ga}_{1-x}\text{Al}_x\text{As}$  as a function of AlAs content," *Applied Physics Letters*, vol. 34, no. 8, pp. 522-524, Apr. 15, 1979.
- [9] S. M. Sze, *Physics of Semiconductor Devices*, 2nd ed., New York: Wiley, 1981.
- [10] G. J. Chaturvedi *et al.*, "Optical effect on GaAs MESFETs," *Infrared Physics*, vol. 23, pp. 65-68, 1983.
- [11] C. Y. Chen *et al.*, "Ultrahigh speed modulation-doped heterostructure field-effect photodetectors," *Applied Physics Letters*, vol. 42, no. 12, pp. 1040-1042, June 15, 1983.
- [12] —, "Modulation-doped  $\text{Ga}_{0.47}\text{In}_{0.53}\text{As}/\text{Al}_{0.48}\text{In}_{0.52}$  as planar photoconductance detectors for 1.0-1.55  $\mu\text{m}$  applications," *Applied Physics Letters*, vol. 43, no. 3, pp. 308-310, Aug. 1, 1983.
- [13] P. C. Claspy and K. B. Bhasin, "Microwave response of a HEMT photoconductive detector," *Microwave and Optical Technology Letters*, vol. 2, no. 1, pp. 1-3, Jan. 1989.
- [14] K. B. Bhasin and R. N. Simons, "Detection of radio-frequency modulation optical signals by two and three terminal microwave devices," in *Technical Symp. Optics, Electro-Optics and Sensors Rec.*, Orlando, FL, May 17-22, 1987.
- [15] H. Rohdin and Roblin, "A MODFET dc model with improved pinchoff and saturation characteristics," *IEEE Trans. Electron Devices*, vol. 33, no. 5, pp. 664-672, May 1986.



**Alvaro A. de Salles** (M'88) was born in Bagé, RGS, Brazil, on March 6, 1946. He received the B.S. degree in electrical engineering from the Federal University of Rio Grande do Sul (UFRGS), Porto Alegre, Brazil, in 1968, the M.Sc. degree in electrical engineering from the Catholic University of Rio de Janeiro (PUC/RJ), Brazil, in 1971, and the Ph.D. degree in electrical engineering from University College, London, England, in 1982.

From 1970 to 1978 he worked as an Assistant Professor at the Catholic University's Center for Research and Development in Telecommunications (CETUC), in Rio de Janeiro, where his major interest was microstrip circulators and filters. From 1978 to 1982 he was at University College London, working on solid-state phased array radar design and on optical control of GaAs MESFET amplifiers and oscillators. From 1982 to 1990 he was at CETUC, doing research and development work on microwave and optical communication semiconductor devices and components. He is presently Visiting Professor at Federal University of Rio Grande do Sul (UFRGS) in Porto Alegre, RS, Brazil.

Dr. de Salles is an Associate Professor at PUC/RJ, and a founding member of the Brazilian Microwave Society (SBMO), and the Brazilian Telecommunications Society (SBT).



**Murilo A. Romero** received the B.Sc. and M.Sc. degrees in 1988 and 1991, respectively, from Catholic University of Rio de Janeiro, Brazil. He is currently pursuing the Ph.D. degree in electrical engineering at the Center for Microwave/Lightwave Engineering at Drexel University, Philadelphia, PA.

His research interests are modeling and simulation of microwave semiconductor devices and study of optical-microwave interactions in solids.

Mr. Romero is a recipient of a scholarship from CNPq (Brazilian Research Council).